Direct Synthesis of Corrugated Superlattices on Non-(100)-Oriented Surfaces

R. Nötzel, N. N. Ledentsov,[a] L. Däweritz,[b] M. Hohenstein,[c] and K. Ploog[d]

Max-Planck-Institut für Festkörperforschung, W-7000 Stuttgart 80, Federal Republic of Germany

(Received 22 January 1991; revised manuscript received 13 November 1991)

We report on the direct synthesis of superlattices with lateral corrugation of the interfaces on (211), (311), and (111) GaAs substrates by molecular-beam epitaxy. Reflection electron diffraction directly shows the formation of arrays of macrosteps during epitaxial growth. High-resolution transmission electron microscopy confirms the transfer of the surface structure to the GaAs/AlAs interface which results in distinct energy shifts in the luminescence of GaAs/AlAs multilayer structures. The surface structure gives rise to lateral quantum-size effects which result in increased exciton continuum energies, in strong exciton-phonon interaction, and in pronounced optical anisotropy.

PACS numbers: 73.20.Dx, 71.35.+z, 78.65.Fa

The study of nanometer-scale phenomena in semiconductors has generated significant interest in both theoretical and experimental physics [1–5]. The most important prerequisite for experimental investigations is the precise fabrication of nanostructured semiconductors. The widely used method of patterning quasi-two-dimensional (2D) heterostructures with nanoscale lithographic techniques introduces defects which often dominate the electronic properties at small dimensions. To reduce the defect densities, several direct fabrication methods based on epitaxial growth have been exploited, including growth of tilted superlattices [6–8], growth on supersteps created due to etching [9], and strain-induced confinement [10,11]. Although the growth of tilted superlattices on vicinal surfaces is considered to be most promising, its successful application has so far been very limited. Apparently the continuous formation of well arranged steps is difficult [7] due to poor control of local misorientation and kink formation.

To overcome the present difficulties associated with the direct fabrication of nanostructured semiconductors [12] we have developed a new approach for the direct synthesis by molecular-beam epitaxy (MBE). The method is based on the *in situ* formation of continuous arrays of macrosteps or facets with a periodicity defined by energy rather than growth-related parameters. At conditions typical for the MBE growth process of (Al,Ga)As, this kind of macrostep can be realized due to the breaking up of a flat surface with high surface energy into facets corresponding to planes with lower surface energy. In this way macrosteps of the desired distance and height are obtained in a reproducible manner.

In this Letter we report on the direct synthesis of GaAs/AlAs multilayer structures with periodic lateral corrugation of the interfaces on GaAs substrates with different crystallographic orientations by MBE. Reflection high-energy electron diffraction (RHEED) directly reveals the formation of asymmetric pyramids on the (211)*B* surface, periodic channels on the (311)*A* surface, and symmetric pyramids on the (111)*A* surface. The transfer of the surface structure to the GaAs/AlAs interface during the growth of GaAs/AlAs multilayer structures is confirmed by high-resolution transmission electron microscopy (HREM). The redshift of the luminescence and the enhancement of the exciton continuum energies are correlated with the height of the surface corrugation. The increased exciton continuum energies directly indicate additional lateral confinement, which is further evidenced by a strong exciton-phonon interaction and a pronounced optical anisotropy. Hence, the observed surface and interface structure offers a unique method to directly synthesize quantum-dot and quantum-wire structures.

The MBE growth on (211)-, (311)-, and (111)-oriented GaAs substrates was monitored by RHEED using a 30-keV electron beam at 1° glancing angle. Seventy-period 46-Å-GaAs/41-Å-AlAs multilayer structures were grown simultaneously on a Mo block with a (100) GaAs substrate as reference. The substrate temperature was 630 °C, the growth rate was 1 μm/h for GaAs and 0.5 μm/h for AlAs, and the As_4/Ga flux ratio was 5. The structural parameters of the samples were determined by double-crystal x-ray diffraction. Photoluminescence (PL) and photoluminescence excitation (PLE) measurements were performed with the samples mounted in an optical He-flow cryostat. Light from a broadband halogen lamp, dispersed by a monochromator, served as the excitation source.

After oxide removal at 580 °C the RHEED patterns of the (211), (311), and (111) surfaces were recorded along different azimuthal directions. The RHEED pattern of the (211) surface shows a reversible faceting of the flat surface at temperatures above 590 °C. The transition occurs continuously over a temperature range between 550 and 590 °C. The observation of the [01$\bar{1}$] azimuth [Fig. 1(a)] exhibits a stepped surface along [$\bar{1}$11] [13]. The lateral periodicity of 9.8 Å ($\triangleq 2a_{111}$) is deduced from the horizontal streak separation and the step height of 2.3 Å from the separation of the intensity maxima along the surface normal. The RHEED pattern along [$\bar{1}$11] [Fig. 1(b)] shows streaks tilted by 30° to the surface normal indicating the presence of {110} facets. As a consequence, the surface comprises two sets of {110} facets along [$\bar{1}$11] and alternating (111) terrace planes and

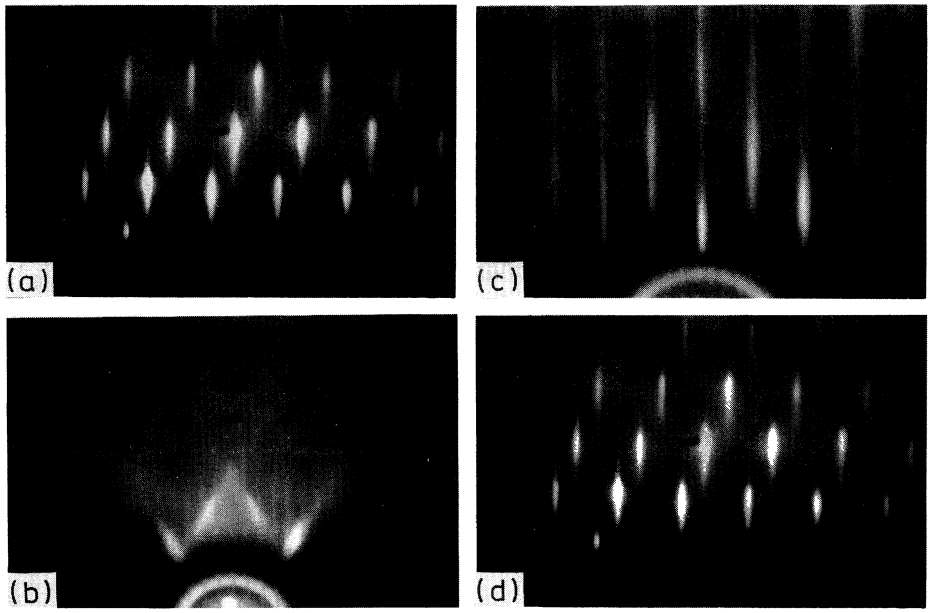

FIG. 1. Reflection high-energy electron-diffraction patterns of the (211) GaAs surface (a) along [01$\bar{1}$], (b) along [$\bar{1}$11], and of the (311) GaAs surface (c) along [01$\bar{1}$], (d) along [$\bar{2}$33].

(100) steps along [01$\bar{1}$] forming asymmetric pyramids of 2.3 Å height ($\triangleq 2d_{211}$).

The RHEED pattern of the (311) surface shows a pronounced streaking along [01$\bar{1}$] indicating a high density of steps along the perpendicular [$\bar{2}$33] direction. Observing the [$\bar{2}$33] azimuth parallel to the steps, the streaks are alternatingly split into sharp satellites or unsplit in dependence on the scattering vector $k_\perp$. This RHEED pattern directly images the reciprocal lattice of an almost perfect two-level system [13]. The separation of the satellites gives the lateral periodicity of 32 Å ($\triangleq 8a_{110}$) for the stepped surface. The extinction of the main streak intensity for maximum intensity on the satellites evidences the high degree of ordering. From the splitting along the streaks the step height is found to be 10.2 Å. These experimental parameters agree perfectly with our model describing the surface as composed of (311) terraces of 4 Å width ($\triangleq 1a_{110}$) and two sets of (33$\bar{1}$) and ($\bar{3}$1$\bar{3}$) facets corresponding to upward and downward steps of 10.2 Å height ($\triangleq 6d_{311}$). In agreement with surface energy considerations [14], the nominal (311) surface breaks up into {331} facets of lower surface energy. The RHEED pattern of the (111) surface shows a distinct splitting along the streaks which is observed along arbitrary azimuthal directions. Hence, this splitting is assigned to the height of the surface corrugation comprising symmetric pyramids of 13.1 Å height ($\triangleq 4d_{111}$).

The RHEED intensity dynamics, described here exemplarily during the growth of (311) GaAs/AlAs multilayer structures, shows a pronounced oscillation at the onset of GaAs and AlAs growth, respectively (Fig. 2). As derived from the respective growth rates, the oscillation corresponds to the deposition of three (311) monolayers, i.e., lattice planes. During the deposition of the next three monolayers, the intensity approaches a value corresponding to the RHEED pattern of the stable stepped surface during growth. This behavior is interpreted as a phase change of the surface corrugation during the deposition of the first six monolayers of GaAs on AlAs and vice versa as illustrated by the upper (shaded) surface in Fig. 3(a), including quasifilling of the corrugation during the first three-monolayer deposition and rearrangement of the stepped surface during the second three-monolayer deposition. We assume that this phase change is induced by strain which plays an important role here and makes the heterogenous growth on the facets energetically less

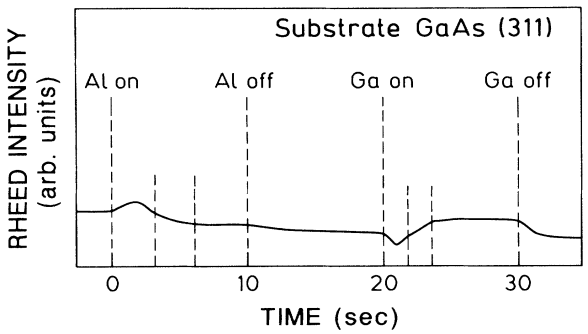

FIG. 2. Reflection high-energy electron-diffraction dynamics during the growth of GaAs/AlAs multilayer structures on (311)-oriented substrates.

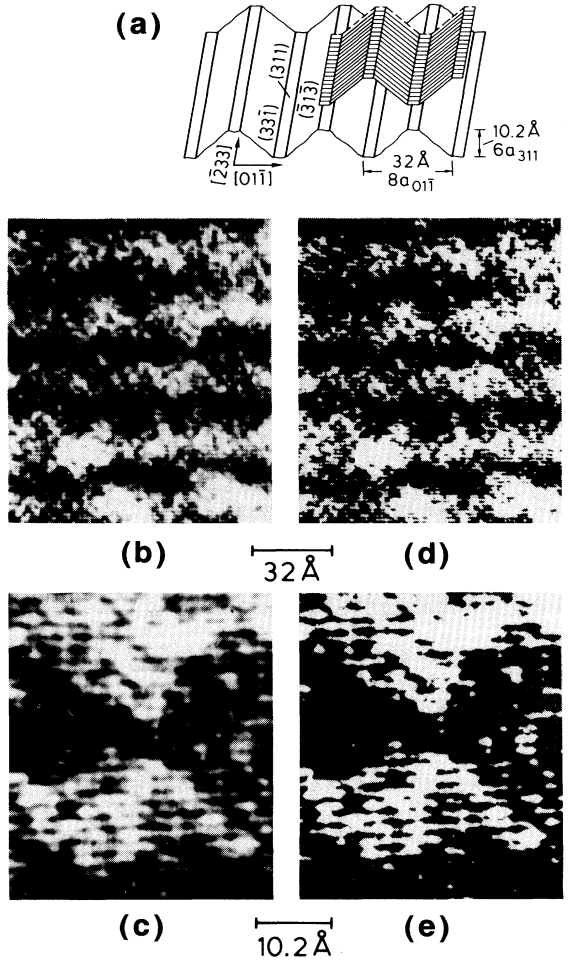

FIG. 3. (a) Schematic of the stepped (311) GaAs surface. The upper surface (shaded) illustrates the phase change of the surface corrugation during the heterogeneous growth of GaAs on AlAs and vice versa. (b),(c) High-resolution transmission electron microscopy image of a 15-Å/13-Å (311) GaAs/AlAs multilayer structure viewed along [2̄33]. In (d),(e) the contrast is enhanced.

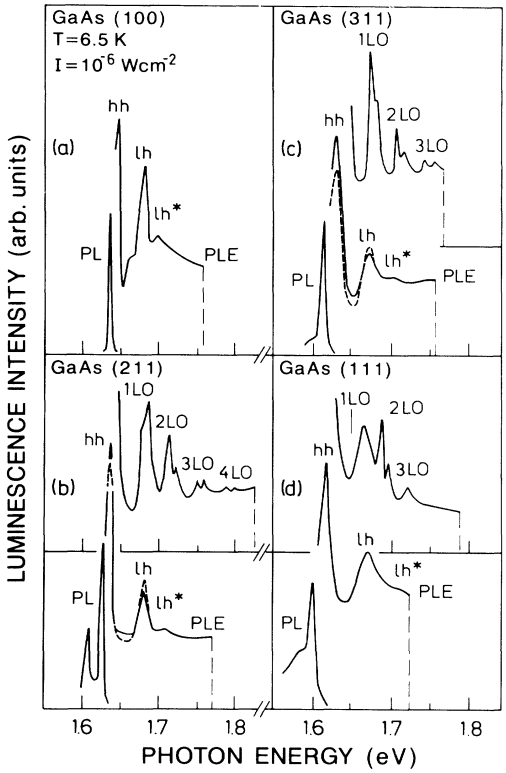

FIG. 4. Photoluminescence (PL) and PL excitation (PLE) spectra of (a) (100), (b) (211), (c) (311), and (d) (111) GaAs/AlAs multilayer structures. For (b) and (c), the dashed lines are for the exciting light polarized parallel to [01 1̄]. The solid lines correspond to the respective perpendicular directions. LO- and TA-phonon related lines are resolved in PLE monitoring the high-energy side of the PL line.

favorable, so that the growth starts upon the low level terrace. As a consequence, the complete structure consists of well ordered alternating thicker and thinner regions of GaAs and AlAs oriented along [2̄33] which form an as-grown lateral superlattice with corrugated interfaces on a nanometer scale.

HREM confirms the existence of alternating thicker and thinner channels along [2̄33] [Figs. 3(b)–3(e)]. Because of unintentional misorientation of the (311) substrates by 1° and the microroughness of the GaAs/AlAs interface the contrast between GaAs and AlAs is not sharp. Nevertheless, the periodic GaAs/AlAs multilayer structures of the present study exhibit a high structural perfection comparable to that of the (100) reference sample and have the same average GaAs and AlAs layer thicknesses as derived from the width, intensity, and separation of the x-ray-diffraction peaks.

The redshift of the PL line with respect to the (100) sample increases with the height of the surface corrugation for the different orientations (Fig. 4 and Table I), reflecting the fact that the luminescence originates from transitions in the respective *thicker* GaAs regions. The observed enhancement of the light-hole (lh) exciton continuum energies (determined from transitions marked by lh* in Fig. 4) also correlates with the height of the surface corrugation (Table I), and indicates additional lateral confinement in the corrugated GaAs/AlAs multilayer structures. The lh character of lh* was proved by the measured negative degree of circular polarization to exclude their origin from "forbidden" transitions. The increased exciton stability is revealed in the strong exciton-phonon interaction due to the high probability for the excitons created above the band gap relaxing as a whole [15,16]. Monitoring the high-energy side of the PL line, strong LO- and TA-phonon related lines are resolved in the PLE spectra of the (311), (211), and (111) samples (Fig. 4). The PLE spectra of the (211) and (311) samples [Figs. 4(b) and 4(c)] exhibit a pro-

TABLE I. Dependence of the luminescence redshift and light-hole (lh) exciton continuum energy on the height of the surface corrugation for various orientations.

Orientation	(100)	(211)	(311)	(111)
Height of the surface corrugation (Å)	0	2.3	10.2	13.1
Redshift of the PL (meV)	0	16	24	38
lh exciton continuum energy (meV)	15	27	29	36

nounced polarization anisotropy of the exciton resonances. This optical anisotropy is in agreement with the asymmetric lateral potential in these structures introduced by the presence of alternating thicker and thinner GaAs and AlAs regions [17,18]. The corresponding polarization behavior is also observed in PL. No optical anisotropy is observed for the (100) and (111) samples as expected for quantum wells and also for the symmetric surface structure of the (111) orientation. The peaked density of states in the (111) sample is revealed in the absence of the 1LO phonon line in PLE [Fig. 4(d)] which coincides in energy with a pronounced minimum in absorption measured above the heavy-hole (hh) state and explains also the observed enhancement of the hh resonance [19].

In summary, we have developed a new method for the direct synthesis of corrugated superlattices which exhibit optical properties characteristic of quantum-wire and quantum-dot structures. During MBE the flat (211), (311), and (111) surfaces break up into regular facets having nanometer-scale dimensions, which was directly monitored by RHEED. In addition, RHEED dynamics has evidenced a unique growth mechanism on the stepped surface. Thicker and thinner regions of GaAs and AlAs are built up, which are confirmed by HREM. Distinct redshifts of the luminescence, enhanced exciton continuum energies, and exciton-phonon interaction evidence lateral confinement in the corrugated GaAs/AlAs multilayer structures. First results show the formation of nanometer-scale structures not limited to the orientations discussed here. Hence, a variety of different structures can be realized also on other crystallographic orientations and material systems, opening a wide field of exciting new phenomena.

This work was supported by the Bundesministerium für Forschung und Technologie of the Federal Republic of Germany.

[a]Permanent address: A. F. Ioffe Physico-Technical Institute, Leningrad, U.S.S.R.
[b]Permanent address: Zentralinstitut für Elektronenphysik, O-1086 Berlin, Federal Republic of Germany.
[c]Permanent address: Max-Planck-Institut für Metallforschung, W-7000 Stuttgart 80, Federal Republic of Germany.
[d]Permanent address: Material Science Department, University of Darmstadt, W-6100 Darmstadt, Federal Republic of Germany.

[1] J. S. Weiner, G. Danan, A. Pinczuk, J. Valladares, L. N. Pfeiffer, and K. West, Phys. Rev. Lett. **63**, 1641 (1989).
[2] E. Kapon, D. Hwang, and R. Bhat, Phys. Rev. Lett. **63**, 430 (1989).
[3] M. A. Reed, J. N. Randall, R. J. Aggarwal, R. J. Matyi, T. M. Moore, and A. E. Wetsel, Phys. Rev. Lett. **60**, 535 (1988); J. Cryst. Growth **95**, 266 (1989).
[4] M. Kohl, D. Heitmann, P. Grambow, and K. Ploog, Phys. Rev. Lett. **63**, 2124 (1989).
[5] M. L. Roukes, A. Scherer, S. J. Allen, H. G. Craighead, R. M. Ruthen, E. D. Beebe, and J. P. Harbison, Phys. Rev. Lett. **59**, 3011 (1987).
[6] M. Tsuchiya, J. M. Gaines, R. H. Yan, R. J. Simes, P. O. Holtz, L. A. Coldren, and P. M. Petroff, Phys. Rev. Lett. **62**, 466 (1989).
[7] T. Fukui and H. Saito, Jpn. J. Appl. Phys. **29**, L731 (1990).
[8] M. Tanaka, J. Motohisa, and H. Sakaki, Surf. Sci. **228**, 408 (1990).
[9] E. Colas, E. Kapon, S. Simhony, H. M. Cox, R. Bhat, K. Kash, and P. S. D. Lin, Appl. Phys. Lett. **55**, 867 (1989).
[10] K. Kash, B. P. Van der Gaag, D. D. Mahoney, A. S. Gozdz, L. T. Florez, J. P. Harbison, and M. D. Sturge, Phys. Rev. Lett. **67**, 1326 (1991).
[11] D. Gershoni, J. S. Weiner, S. N. G. Chu, G. A. Baraff, J. M. Vandenberg, L. N. Pfeiffer, K. West, R. A. Logan, and T. Tanbun-Ek, Phys. Rev. Lett. **65**, 1631 (1990).
[12] E. Corcoran, Sci. Am. **263**, 74 (1990).
[13] M. G. Lagally, D. E. Savage, and M. C. Tringides, in *Reflection High-Energy Electron Diffraction and Reflecting Electron Imaging of Surfaces*, edited by P. K. Larsen and P. J. Dobson, NATO Advanced Study Institutes, Ser. B (Plenum, New York, 1988), p. 139.
[14] D. J. Chadi, Phys. Rev. B **29**, 785 (1984).
[15] S. Permogorov, Phys. Status Solidi (b) **68**, 9 (1975).
[16] R. Nötzel, N. N. Ledentsov, L. Däweritz, K. Ploog, and M. Hohenstein, Phys. Rev. B (to be published).
[17] P. C. Sercel and K. J. Vahala, Appl. Phys. Lett. **57**, 545 (1990).
[18] D. S. Citrin and Y. C. Chang, Phys. Rev. B **43**, 11703 (1991).
[19] T. Hayakawa, K. Takahashi, M. Kondo, T. Suyama, S. Yamamoto, and T. Hijikata, Phys. Rev. Lett. **60**, 349 (1988).

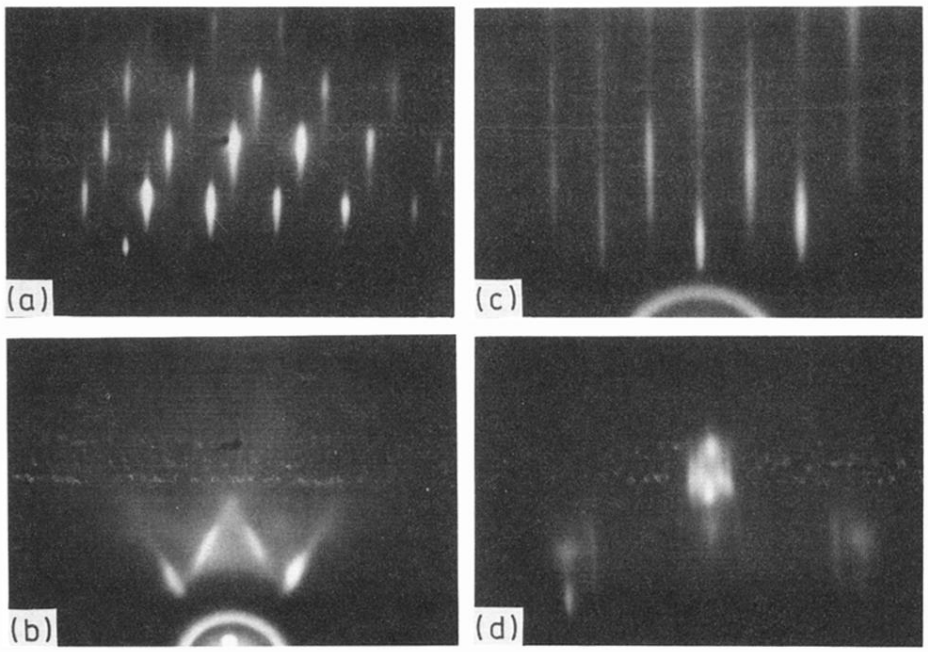

FIG. 1. Reflection high-energy electron-diffraction patterns of the (211) GaAs surface (a) along [01$\bar{1}$], (b) along [$\bar{1}$11], and of the (311) GaAs surface (c) along [01$\bar{1}$], (d) along [$\bar{2}$33].

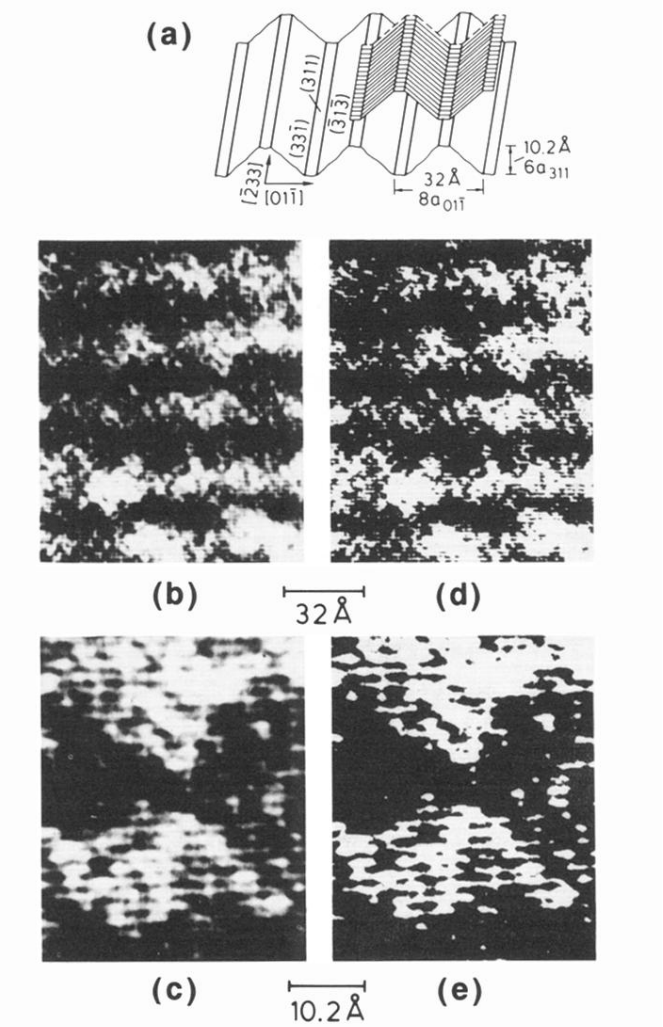

FIG. 3. (a) Schematic of the stepped (311) GaAs surface. The upper surface (shaded) illustrates the phase change of the surface corrugation during the heterogeneous growth of GaAs on AlAs and vice versa. (b),(c) High-resolution transmission electron microscopy image of a 15-Å/13-Å (311) GaAs/AlAs multilayer structure viewed along [$\bar{2}$33]. In (d),(e) the contrast is enhanced.